CFD MODELLING OF NON-ISOTHERMAL PROTON EXCHANGE MEMBRANE FUEL CELL (PEMFC): ROLE OF BAFFLES

Ashraf Ali Basheer, Naveen Ganta

Complex Fluid Flow and Visualization Research Lab
Department of Chemical Engineering
National Institute of Technology Karnataka
Surathkal, Karnataka, India - 575025
E-mail: ashrafali@nitk.edu.in

Received 10 February 2023
Accepted 08 August 2023
DOI: 10.59957/jctm.v59.i4.2024.26

ABSTRACT

Through oxidation (H_2) and reduction (O_2) reactions, the chemical energy of the fuel is converted by proton exchange membrane fuel cell (PEMFC) into electricity and is therefore considered an energy converter. In this work, performance of a PEMFC is numerically investigated using computational fluid dynamics (CFD). To characterize the non-isothermal behavior of PEMFC, 3D transient CFD simulations are performed. The distribution of H_2 and O_2 mass fractions, temperature, and current density profiles are analyzed for various operational conditions. The optimum condition (voltage = 0.1 V; thickness of gas diffusion layer (GDL) = 0.0127mm; thickness of catalyst layer (CL) = 0.014mm) for an operation of PEMFC is identified Trapezoidal and rectangular baffles are proposed into the flow channels to enhance the performance of PEMFC. The rectangular baffle configuration supports maximum conversion of reactant gases (H_2 = 24.16 %, O_2 = 41.72 %) in comparison with the trapezoidal baffle. A significant increase in conversion is reported when the number of baffles in the gas flow channel is increases. Thus, PEMFC performance is enhanced with baffle configuration.

Keywords: Proton Exchange Membrane Fuel Cell (PEMFC), Non-isothermal, Baffle, CFD.

INTRODUCTION

PEMFCs are electrochemical energy device which converters fuel's chemical energy directly into electricity. This device requires a constant supply of fuel and oxidants for its functioning. CFD models are extensively used to design and characterize single channel PEMFC. Springer et al. characterized performance of PEMFC using a 1D isothermal, steady-state model [1]. The ratio of net water per H^+ flux is found to be $1/10^{th}$ of the electro-osmotic drag coefficient when a hydrated membrane is used.

The impact of operating factors on PEMFC performance was examined by Wang et al. [2]. The operating temperature and pressure were found to be crucial factors in improving PEMFC performance. Ju et al. found that thermal effects are significant at lower gas diffusion layers and higher current density [3]. A 3D, CFD model (non-isothermal) was used by Baca et al. to predict the flow behavior of single-channel PEMFC and non-uniform current density was found across the catalyst layer [4]. A 3D, non-isothermal model was developed by Wu et al. to investigate the water transport mechanism in PEMFC [5]. In this study, it was found that performance of PEMFC was affected by rates of sorption and desorption of H_2O which is in membrane, capillary pressure, and permeability.

Hashemi et al. characterized the performance of straight and serpentine PEMFC using non-isothermal, 3D models and found that temperature distribution as well as current density distribution was higher in serpentine flow channels [6]. The performance of straight gas flow channel was compared with serpentine flow channel [7]. They found that temperature distribution was uniform

in serpentine flow PEMFC. A 3D (isothermal), CFD model was developed and the significance of membrane thickness on PEMFC performance was studied [8].

M. Kaplan found that an optimal membrane thickness is necessary to enhance cell efficiency. He achieved significant cell performance with a lower membrane thickness [9]. F. Mojica et al. have studied extensively by considering various flow designs of PEMFC by varying relative humidity (RH) and flow stoichiometry. They found that the performance of fuel cell improved when RH and flow stoichiometry was increased [10]. The significance of multiple serpentine channels on PEM fuel cell performance was analysed and it was found that channel and width significantly affect PEM performance [11]. H. Askaripour characterized two-phase flow behavior in PEMFC and found that operating conditions such as inlet RH, stoichiometry, pressure, and temperature significantly affect cell performance [12]. M. G. Waller et al. found that PEMFC performance was enhanced by increasing pressure and temperature [13].

Amadane et al. characterized performance of the PEMFC using a thermo-fluid model. They found that the distribution of H_2 and H_2O is influenced by operating cell voltage [14]. Wilberforce et al. characterized the performance of PEMFC using a 3D (isothermal) model for various bipolar plate materials [Al, Cu and Stainless steel (SS)] [15]. They found that the Aluminium (Al) bipolar plate significantly improves cell performance. The importance of operating parameters such as pressure and temperature on the performance of PEMFC was analyzed [16]. They found that operating pressure and temperature are significant parameters in improving cell performance. A tapered flow configuration in PEMFC which supports uniform water saturation over the surface of the catalyst layer (CL) was proposed by Ghasabehi et al. [17]. A 3D (non-isothermal) CFD model was developed by Xia et al. and studied the significance of the thickness of the membrane and porosity (gas diffusion layer) on flow uniformity, diffusion flux, and ohmic resistance was studied [18]. They found that thickness and porosity are significant parameters in characterizing the performance of PEMFC.

In most of the published literature on PEM fuel cells, performance of PEMFC is enhanced by changing operational parameters (pressure, temperature, inlet mass fraction of fuel, etc.) and geometrical parameters (thickness of catalyst layer (CL), gas diffusion layer (GDL), and membrane, etc.). But in very few literatures, obstacles (baffles) were used to enhance the flow field in PEMFC fuel cells. To the best of our knowledge, the configuration of obstacles (baffles) and their implication on the flow field and reaction are not reported in the literature. Hence, in the present work, baffles are introduced into the gas flow channel to enhance the performance of PEMFC. To predict the flow behavior and to assess the performance of a single-channel PEMFC, transient 3D CFD simulations are carried out.

The geometry of the PEMFC is described first in this article. Following that, the transport equations and procedures used for CFD calculation are discussed. The numerically predicted results are analyzed and presented in the results and discussion. Finally, the key findings are summarized.

Schematic of Proton Exchange Membrane Fuel Cell (PEMFC)

Fig. 1 depicts schematic of the PEMFC. It includes current collectors (anode and cathode), flow channels, GDL, CL, and membranes. ANSYS Workbench 2022 R1 is used to develop geometry of PEMFC using hexahedral mesh elements.

CFD Modelling

The continuity, momentum, energy, the concentration of species, and charge transport (Joule heating reaction, Butler-Volmer & Nernst) equations are solved to characterize the transport processes occurring in CL, GDL, membrane, and flow channels. CFD model is developed with the assumptions that inlet gases follow ideal gas behavior, flow is laminar, H_2O exists as a gas phase, membrane materials are isotropic, catalyst and gas diffusion layer, and thermo-physical properties are constant.

The transport equations are given as

Continuity equation

$$\nabla.(p\vec{v}) = S_m \tag{1}$$

Momentum equation

$$\nabla.(\rho\,\vec{v}\;\vec{v}) = -\nabla p + \nabla.(\mu^{eff}\nabla\vec{v}) + S_p \tag{2}$$

The porous media characteristics are incorporated through the source term (S_p),

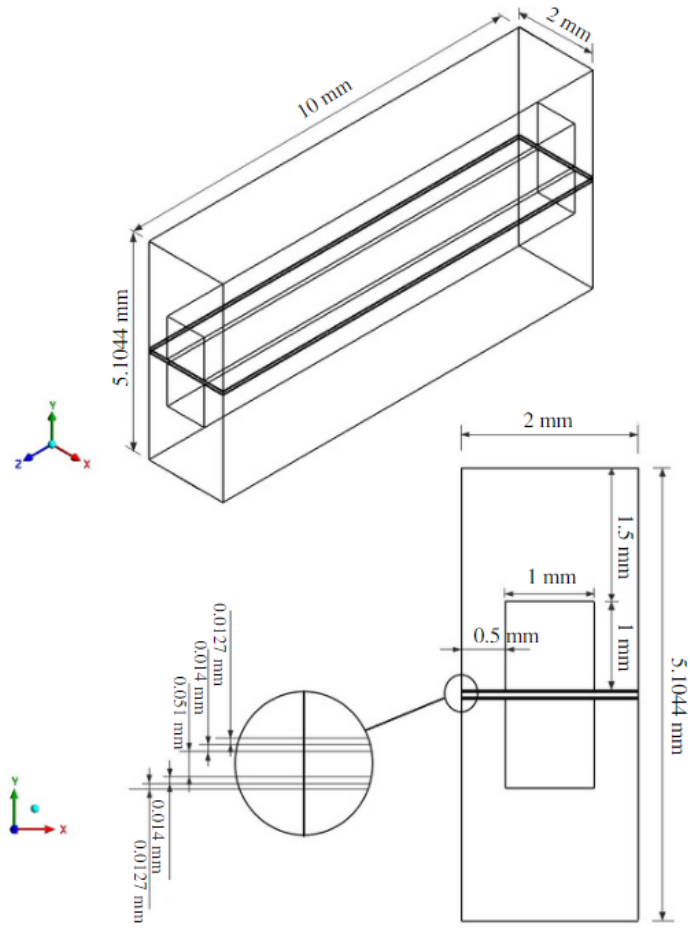

Fig. 1. Schematic of PEMFC.

$$S_p = -\left(\frac{\mu}{k}\right)\vec{v} \quad (3)$$

Species transport equation

$$\nabla.(\rho\,\vec{v}\,y_i) = -\nabla.\overrightarrow{J_i} + S_i \quad (4)$$

The diffusive flux for the species i ($\overrightarrow{J_i}$) is obtained using,

$$\overrightarrow{J_i} = -\rho D_i \nabla.y_i \quad (5)$$

Energy balance equation

$$\nabla.[\vec{v}(\rho E + p)] = \nabla.(K_{eff}\nabla T - \Sigma_i h_i \overrightarrow{J_i}) \quad (6)$$

The transport equations (1-6) along with charge equations are solved to characterize performance of PEMFC. The detailed transport equations are obtained from literature [19, 20].

Simulation Methodology

The PEMFC is modeled using ANSYS Workbench 2021 R1 using hexagonal mesh elements. 3D CFD simulations are performed to characterize the performance of PEMFC. The mesh independence analysis is carried out to ensure CFD predictions are independent of mesh size (optimum: 1.5 Lakhs). The velocity inlet boundary condition (BC) which is set at inlet (cathode and anode) and pressure outlet BC which is set at outlet (cathode and anode). At the fuel cell terminals (cathode and anode), electrical BC is specified. The pressure and velocity fields are computed using the SIMPLE algorithm on a staggered grid. The convergence criteria (10^{-6}) is set for all the transported variables. The resistance in the various

components of PEMFC is accounted for, through Joule heating. The generation of heat due to chemical reaction in PEMFC is considered in reaction heating models, and the electrochemistry that occurs in fuel cell is accounted for as a source term in the transport equations. The current transfer across the catalyst layers is predicted using Butler-Volmer rate. The water transport within the membrane, conductivity and diffusion rate within the GDL is accounted through CFD model.

RESULTS AND DISCUSSION

According to the operating circumstances listed in Table 1, 3D transient CFD simulations are carried out to predict the flow in the PEMFC. The predicted current density distribution across the GDL and catalyst layer is analyzed for various operating voltages (0.1 - 1.0 V, Fig 2). At lower operating voltages, the current density is observed to be high, and as voltage rises, the current

Table 1. Operating conditions for proton exchange membrane (PEM) fuel cell.

Parameters	Value
Anode and Cathode (inlet temperature)	343 K
Inlet flow velocity of gases (anode/cathode)	0.2 m s^{-1}
Operating pressure	303975 Pa
Mass fractions (anode) of H_2 and H_2O (vapor)	0.8/0.2
Mass fractions (cathode) of O_2 and H_2O (vapor)	0.8/0.2
Relative humidity (Anode)	100 %
Relative humidity (Cathode)	100 %
Circuit voltage (Open)	1.05 V

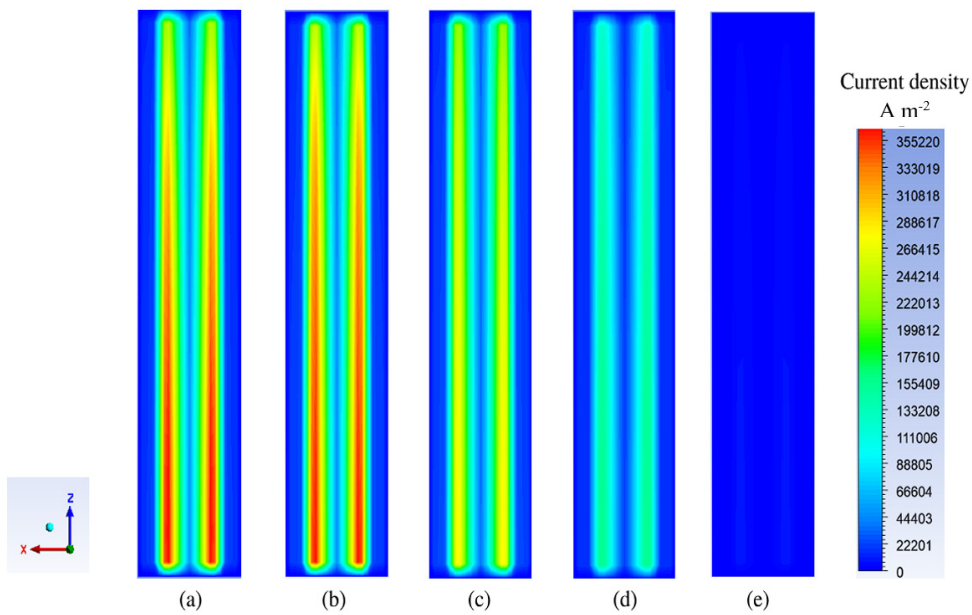

Fig. 2. Contours of current density distribution (anode) at the interface between GDL/CL (Y = 2.54mm, parallel to ZX plane) for (a) 0.1V (b) 0.3V (c) 0.5V (d) 0.7V (e) 1.0V.

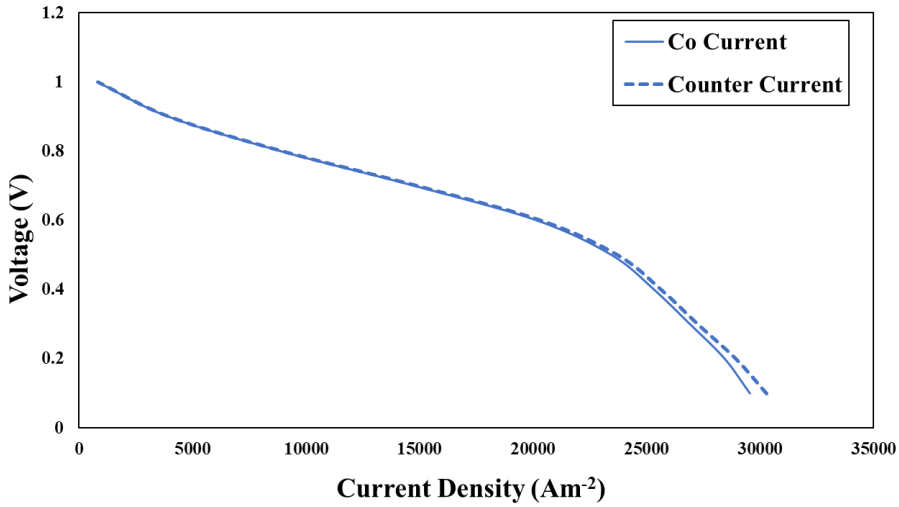

Fig. 3. Effect of mode of operation on polarization curve.

density value drops. This is attributed to the extent of conversion of fuel with O_2.

The predicted polarization curves [current density as a function of cell potential (voltage)] are inquired for co-current and counter-current modes of operation (Fig. 3) to characterize the performance of PEMFC. The polarization curve shows three distinct regions (low, moderate, and high current density regions). The sharp drop in voltage is observed at the initial stage (low current density region) due to activation loss. The linear decrease in voltage loss is observed at moderate current density regions due to ohmic loss (i.e. resistance offered by the membrane and components of the fuel cell for the flow of H^+ ions). A significant drop in voltage is observed at high current density regions due to the rapid consumption of reactants at the electrode surface (concentration loss). Since predicted polarization profiles for both co-current and counter-current modes of operation in low current density zones are found to be the same, co-current mode of operation is chosen for further investigation.

To find an optimum cell potential (voltage) for the operation of PEMFC, the predicted contours of H_2 mass fraction (anode) distribution for various operating voltages (Fig. 4) are analyzed. The H_2 mass fraction distribution is found to decrease along the flow channel length due to fuel consumption (H_2) at the anode catalyst layer. The maximum mass fraction of H_2 was observed at the flow channel inlets (minimum at the outlets of the flow channel). At higher voltage, due to lower fuel (H_2) consumption, the hydrogen mass fraction at the exit is observed to be high.

Fig. 5 depicts the distribution of O_2 mass fraction across the flow channel. It is found that the mass percentage of oxygen along the length of the channel decreases reaching maximum value at the inlet of flow channel and minimum value at the outlet of the flow channel respectively. As the voltage increases, the extent of consumption of O_2 also increases along the flow channel. Thus, the driving force for the movement of O_2 is decreases across catalyst layer (CL) and the gas diffusion layer (GDL). This leads to more O_2 consumption at lower cell voltage (high current density).

To quantitatively investigate the performance of PEMFC, a line is chosen at Y = 2.506 mm (parallel to ZX plane) and current density distribution across the GDL/CL layer (cathode) is analyzed for different H_2 mass fraction (inlet). This is depicted in Fig. 6. It has been found that there is a high local current density distribution at the inlet of the flow channel and low current density distribution at the flow channel inlets. Hence, across GDL/CL interface reactant concentration was found to decrease. As fuel concentration (H_2) increases, the current density increases, and its magnitude is found

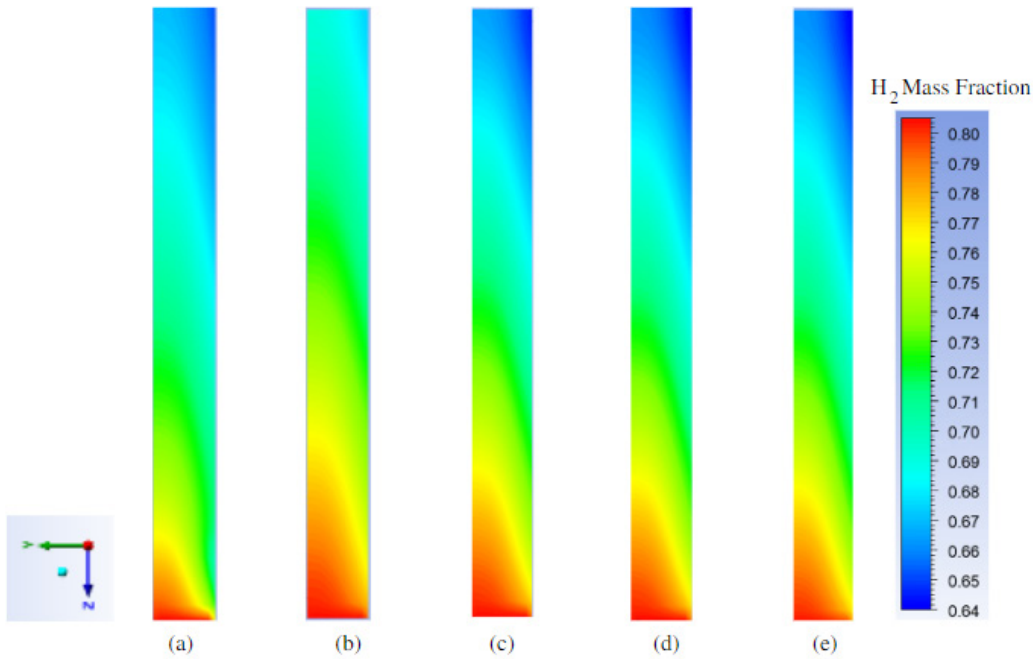

Fig. 4. Contours of H_2 mass fraction distribution in the anode channel for (a) 0.1V (b) 0.3V (c) 0.5V (d) 0.7V (e) 1.0V.

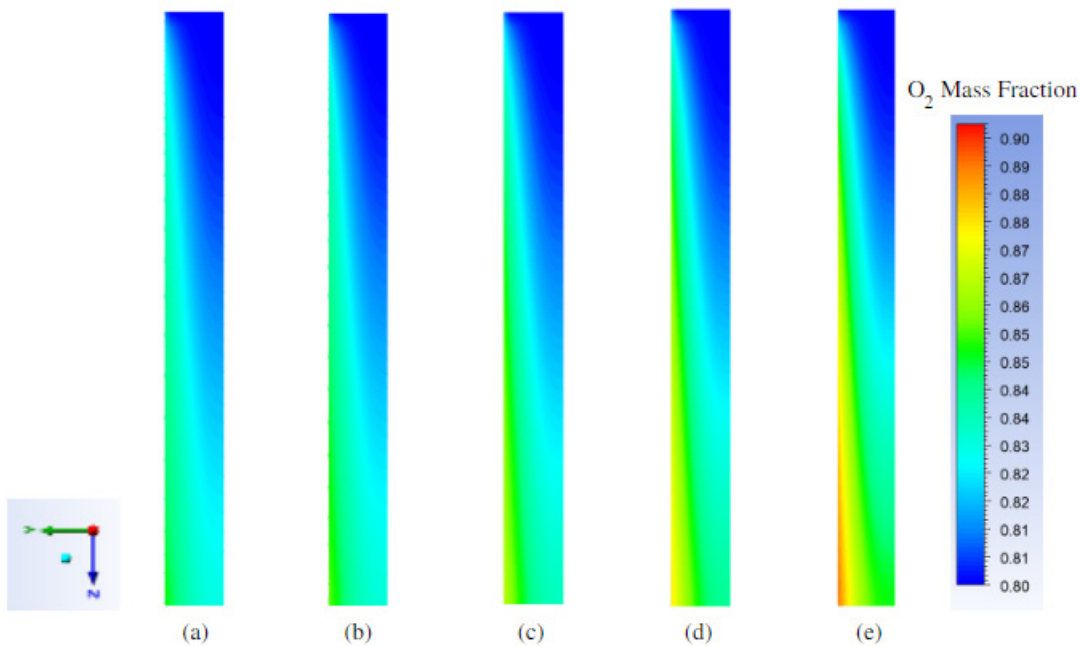

Fig. 5. Contours of O_2 mass fraction distribution in the cathode channel for (a) 0.1V (b) 0.3V (c) 0.5V (d) 0.7V (e) 1.0V.

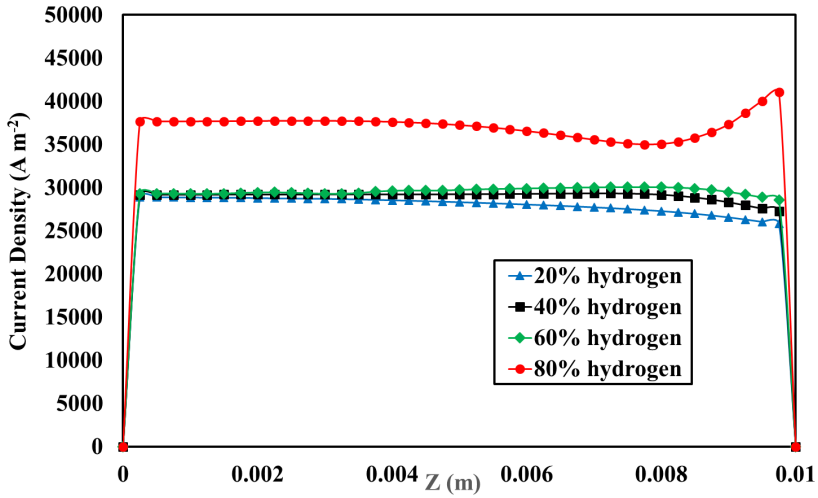

Fig. 6. Effect of H_2 mass fraction on the current density distribution across cathode GDL/CL interface.

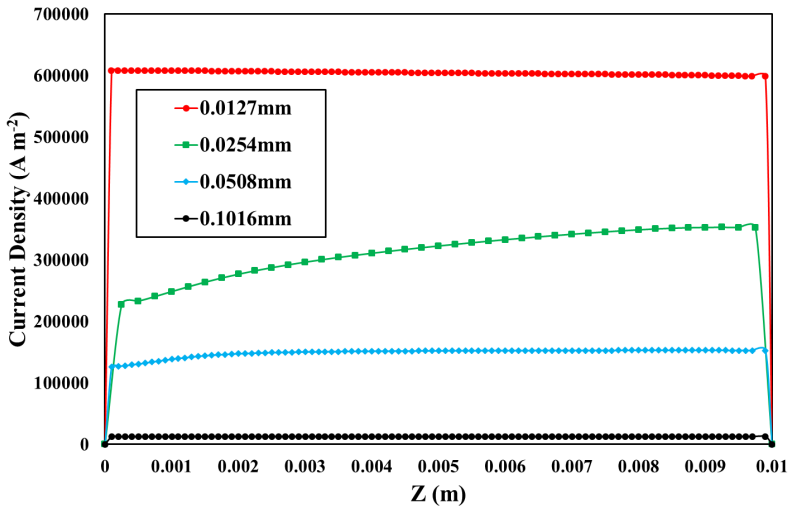

Fig. 7. Effect of GDL thickness on the current density distribution across cathode GDL/CL interface.

to be maximum when 80 % H_2 mass fraction is used. This is attributed to availability of H_2 in the reaction environment.

In the present study, electrical properties of GDL and the thickness of GDL are taken into consideration to characterize the performance of PEMFC as it significantly influences heat, mass transport and of the fuel cell. Accordingly, various GDL thicknesses are considered and their effect on fuel cell performance are analyzed. This is shown in Fig. 7. Fuel cell potential (performance) is observed to be increasing when the GDL thickness decreases. Since thinner GDL allows more distribution of gaseous reactants over the CL, the extent of current density produced by PEMFC increases.

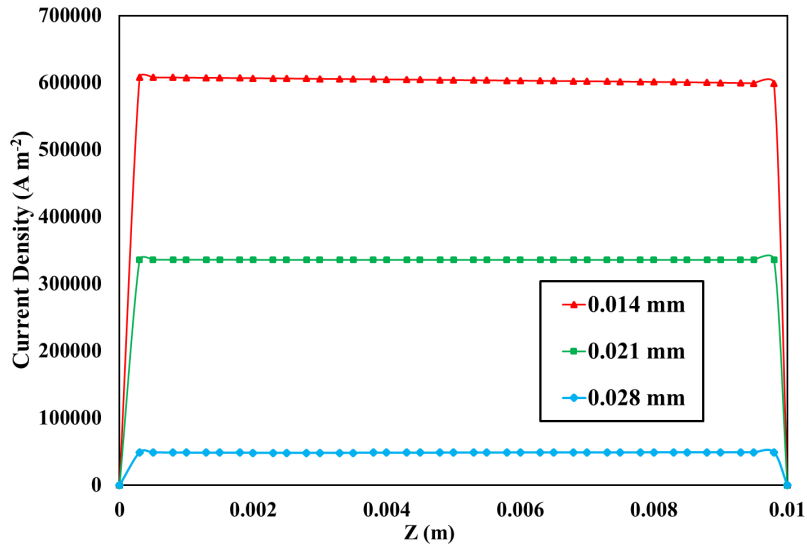

Fig. 8. Effect of CL thickness on the current density distribution across the cathode GDL/CL interface.

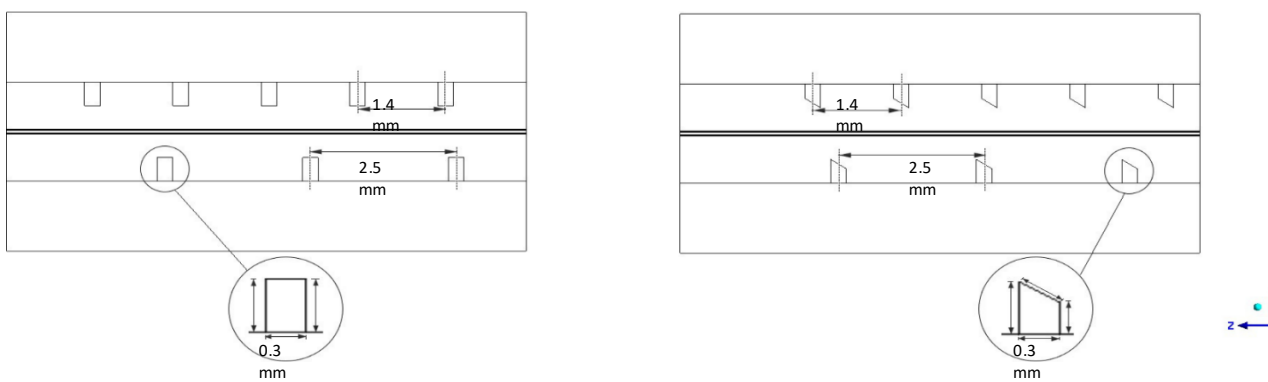

Fig. 9. Flow channel modifications using (a) rectangular baffle and (b) trapezoidal baffle.

The current density produced by PEMFC is maximum when GDL thickness of 0.0127 mm (thinner) is used and it is thus considered to be the optimum GDL thickness for the operation of PEMFC.

To improve the performance of PEMFC, various catalyst layer (CL) thicknesses (0.014 - 0.028 mm) are considered and optimum catalyst layer (CL) thickness is identified that improves electrochemical performance (strength) of PEMFC (Fig. 8). The magnitude of current density is found to be high when thinner CL (0.014 mm) is used. This is due to the extent of proton conductivity resistance (low) offered by thinner CL. Thus, thinner membrane supports in enhancing fuel cell performance.

To further enhance the PEMFC performance, obstacles (trapezoidal and rectangular baffles) are proposed for the cathode and anode gas flow channels. The obstacle configuration is shown in Fig. 9. The corresponding flow field is shown in Fig. 10 and compared with the straight gas flow channel (conventional). It is observed that obstacles (rectangular and trapezoidal baffles) enhance the characteristics of PEMFC by changing area of cross section of the flow channel. This leads to abrupt variations in local current density distribution. Consequently, the oxygen

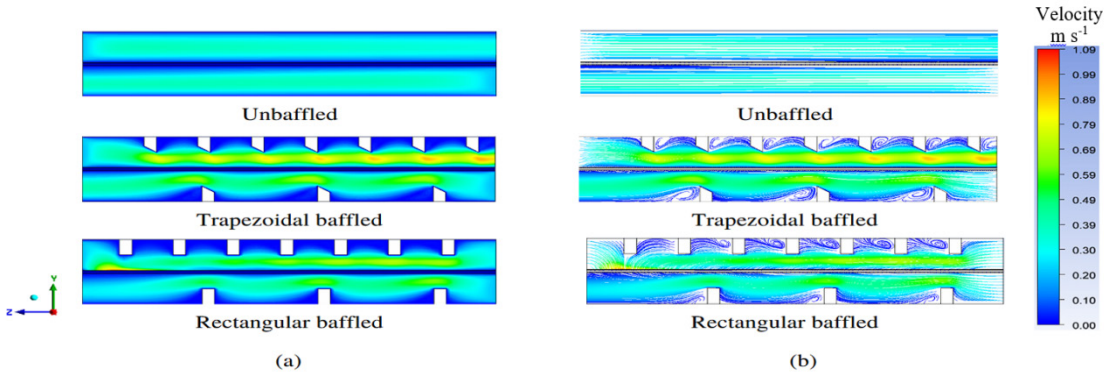

Fig. 10. Performance of flow channel obstacles (x = 1 mm, parallel to YZ plane) (a) contours of velocity magnitude (b) velocity streamline.

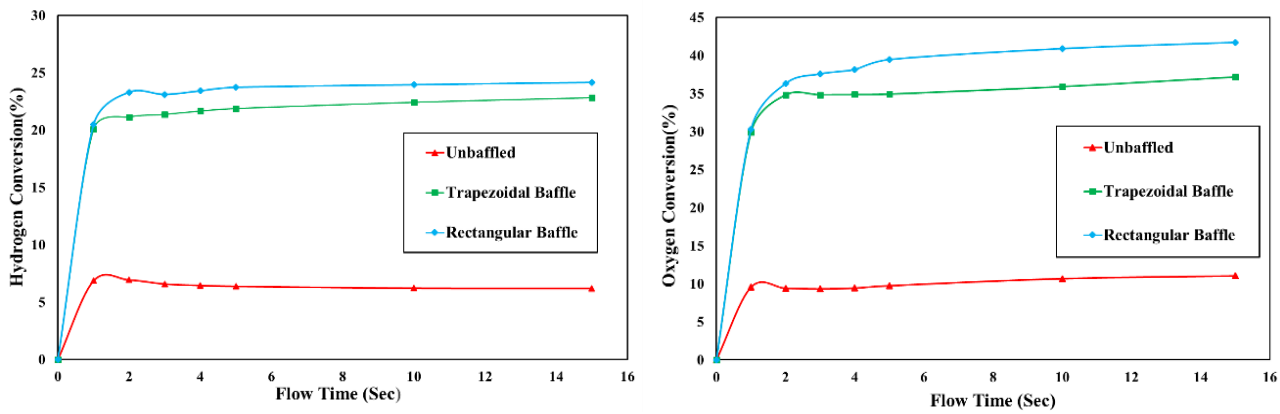

Fig. 11. Effect of baffle configuration on (a) H_2 conversion (%) and (b) O_2 conversion (%) of PEM flow channel.

and hydrogen consumption within the flow channel has increased (Fig. 11) when baffled PEM (trapezoidal and rectangular) is used. The predicted conversion is found to be almost four times higher (rectangular baffle: H_2 = 24 %, O_2 = 42 % and trapezoidal baffle: H_2 = 23 %, O_2 = 37 %) than unbaffled fuel cell system (H_2 = 6. %, O_2 = 11 %). This is attributed to the obstacles (baffles) in the gas flow channel, and it enhances gas flow circulation as velocity of reactant gases increases. Accordingly, the extent of conversion is found to be high when baffles are introduced into the flow domain. Hence baffle configuration supports in improving performance of PEMFC.

Further, the number of baffles in the anode (for fixed 3 baffles in cathode section) and cathode flow channel (for fixed 3 baffles in anode section) are varied. Its effects on flow channel's conversion of H_2 and O_2 are determined. This is shown in Fig. 12 a-b. The conversion of hydrogen and oxygen increases when the number of baffles is increased at anode and cathode respectively. This is due to enhanced circulation in the flow field when the number of baffles in the flow channel are increased. Thus, the PEM fuel cell performance was enhanced by addition of number of baffles to the flow channel.

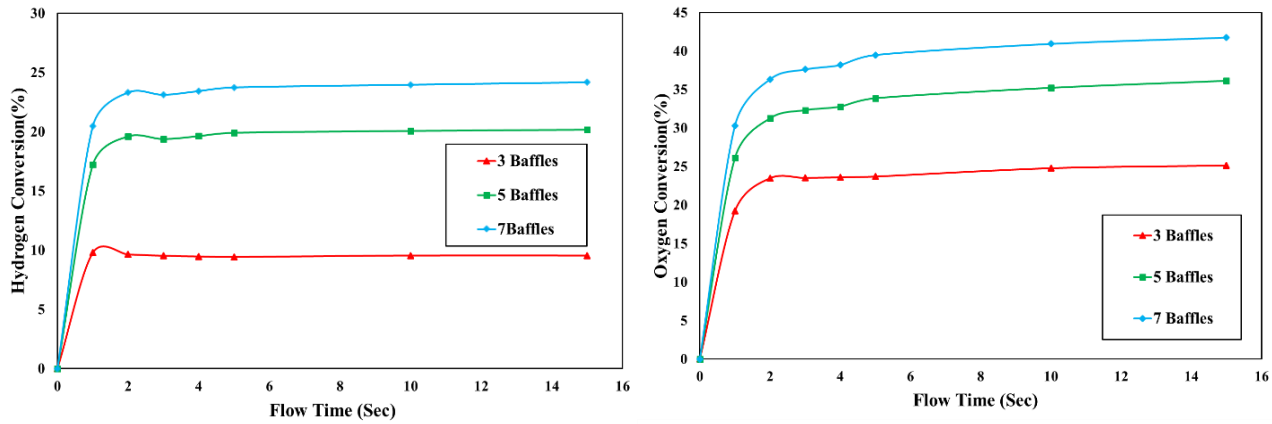

Fig. 12. Effect of number of baffles on (a) H_2 conversion (%) and (b) O_2 conversion (%) of PEM flow channel.

CONCLUSIONS

To characterize PEMFC performance, a non-isothermal 3D CFD model is developed. The predicted polarization curve is analyzed for co-current and counter current modes of operations. The polarization curve is found to be the same in low current density region between the modes of operations of PEMFC. The co-current mode of operation is considered to be suitable mode of operation. The extent of current density distribution for various H_2 mass fractions (inlet) is analyzed to characterize the performance of PEMFC. The predicted current density is found to be high when 80 % H_2 mass fraction is used. Further, the importance of GDL thickness is analyzed and the current density produced by PEMFC is found to be high when thinner GDL thickness (0.0127 mm) is used. The performance of PEMFC is further investigated with changing CL thickness. When using thinner CL (0.014 mm), it is discovered that the current density is high. The conversion of reactant gases is found to be high at lower operating potential. The current density decreases with increasing potential, decreasing the thickness of GDL and CL, thus enhancing the performance of PEM fuel cell. Further, baffles (trapezoidal and rectangular) are introduced in the flow channel. The rectangular baffles are found to be superior in improving the conversion of reactant gases [H_2 (24 %) and O_2 (41 %)] due to enhanced flow velocity in PEMFC. Also, an increase in conversion of reactant gases is observed when number of baffles in the flow channel is increased. Thus, baffled PEM fuel cell configuration with thin GDL and thin CL supports increasing performance of PEMFC.

Acknowledgements

The authors express their gratitude to Mr. Aarif A. for his support in drafting the manuscript.

Nomenclature

$\frac{\partial C}{\partial z}$	concentration gradient
C_{cl}	concentration in catalyst layer
$C_{channel}$	concentration in channel
S	area of cross section
ρ	gas density
D	coefficient of diffusion for species i
$\vec{J}_i$	diffusive flux of species i
D	diffusion coefficient, $m^2\ s^{-1}$
K_{eff}	effective conductivity
K	effective conductivity, $W\ m^{-1}\ K^{-1}$
μ^{eff}	effective viscosity (gas mixture)
h	enthalpy, J
j	exchange current density, $A\ m^2$
F	Faraday constant, 96,487 $C\ mol^{-1}$
J	flux diffusion, $kg\ m^2\ s^{-1}$
μ	gas viscosity ($kg\ m.s^{-1}$)
L	length of conductor
y	mass fraction species
K	permeability (catalyst layers & gas diffusion

layers)

k	permeability, m^2
p	pressure, Pa
r	resistivity
p	static pressure
S_m	source term
S_i	source term for species i
T	temperature, K
δ_{gdl}	thickness of gas diffusion layer
E	total energy
R	transfer current, A m^{-3}
R	Universal gas constant, 8.314 J K^{-1} mol^{-1}
$\vec{v}$	gas velocity
υ	velocity, ms^{-1}
a	water activity

Greek symbols

Ø	cell potential, V
γ	concentration coefficient
ρ	density, kg m^{-3}
μ	dynamic viscosity, kg m^{-1} s^{-1}
σ	electric or ionic conductivity, $ohm^{-1}m^{-1}$
η	over-potential, V
α	transfer coefficient
λ	Water content

Subscripts/superscripts

an	anode
ca	cathode
eff	effective
m	mass
mem	membrane
p	porous
ref	reference
sol	solid

REFERENCES

1. T.E. Springer, T.A. Zawodzinski, S. Gottesfeld, Polymer electrolyte fuel cell model, J. Electrochem. Soc., 138, 1991, 2334-2342.
2. L. Wang, A. Husar, T. Zhou, H. Liu, A parametric study of PEM fuel cell performances, Int. J. Hydrogen Energy, 28, 2003, 1263-1272.
3. H. Ju, H. Meng, C.Y. Wang, A single-phase, non-isothermal model for PEM fuel cells, Int. J. Heat Mass Transf., 48, 2005, 1303-1315.
4. C.M. Baca, R. Travis, M. Bang, Three-dimensional, single-phase, non-isothermal CFD model of a PEM fuel cell, J. Power Sources, 178, 2008, 269-281.
5. H. Wu, X. Li, P. Berg, On the modeling of water transport in polymer electrolyte membrane fuel cells, Electrochim. Acta, 54, 2009, 6913-6927.
6. F. Hashemi, S. Rowshanzamir, M. Rezakazemi, CFD simulation of PEM fuel cell performance: effect of straight and serpentine flow fields, Math. Comput. Model., 55, 2012, 1540-1557.
7. I. Zaman, B. Manshoor, A. Khalid, L.A.M. Sterand, S.W. Chan, Effects of Straight and Serpentine Flow Field Designs on Temperature Distribution in Proton Exchange Membrane (PEM) Fuel Cell, in MATEC Web of Conferences, 2016, 78, 1116.
8. P. Kahroba, I. Mirzaee, H. Shirvani, The Influence of Membrane thickness on the PEM Fuel Cell Operation, 2009.
9. Y. Amadane, H. Mounir, A. Elmarjani, E.M. Karim, Numerical investigation of hydrogen consumption in Proton Exchange Membrane Fuel Cell by using computational fluid dynamics (CFD) simulation, Mediterr. J. Chem., 7, 2019, 396-415.
10. M. Kaplan, Three-dimensional CFD analysis of PEMFC with different membrane thicknesses, Renew. Energy Sustain. Dev., 8, 2022, 45-51.
11. F. Mojica, M. A. Rahman, J. M. Mora, J. D. Ocon, P. Chuang, Experimental study of three channel designs with model comparison in a PEM fuel cell, Fuel Cells, 20, 2020, 547-557.
12. E. Carcadea, M. Varlam, M. Ismail, D.B. Ingham, A. Marinoiu, M. Raceanu, C. Jianu, L. Patularu, D. Ion-Ebrasu, PEM fuel cell performance improvement through numerical optimization of the parameters of the porous layers, Int. J. Hydrogen Energy, 45, 2020, 7968-7980.
13. H. Askaripour, Effect of operating conditions on the performance of a PEM fuel cell, Int. J. Heat Mass Transf.,144, 2019, 118705.
14. M.G. Waller, M.R. Walluk, T.A. Trabold, Performance of high temperature PEM fuel cell materials. Part 1: Effects of temperature, pressure and anode dilution, Int. J. Hydrogen Energy, 41, 2016, 2944-2954.
15. T. Wilberforce, O. Ijaodola, O. Emmanuel, J. Thompson, A.G. Olabi, M.A. Abdelkareem, E.T. Sayed, K. Elsaid, H.M. Maghrabie, Optimization of fuel cell performance using computational fluid

dynamics, Membranes (Basel), 11, 2021, 146.
16. A. Awan, M. Saleem, A. Basit, Simulation of Proton Exchange Membrane Fuel Cell by using ANSYS Fluent, IOP Conference Series: Materials Science and Engineering, 414, 2018, 012045.
17. M. Ghasabehi, M. Ashrafi, M. Shams, Performance analysis of an innovative parallel flow field design of proton exchange membrane fuel cells using multiphysics simulation, Fuel, 285, 2021, 119194.
18. L. Xia, M. Ni, Q. Xu, H. Xu, K. Zheng, Optimization of catalyst layer thickness for achieving high performance and low cost of high temperature proton exchange membrane fuel cell, Appl. Energy, 294, 2021, 117012.
19. ANSYS Fluent 17.0 Advanced addon-modules, 2016, ANSYS Inc., USA.
20. ANSYS Fluent 18 Tutorial Guide, 2017, ANSYS Inc., USA.